Volume 14, Issue 3, 142426 (1-13)

Iranian Journal of Catalysis (IJC)

https://doi.org/10.57647/j.ijc.2024.1403.26

Synthesis and application of new Co/Cu/Ni/Zn (II) Schiff base complexes in the biological activity and oxidation of alcohols

Teeba Khalid Adnan, Khansa Yousif Ahmed , Areej Ali Jarullah*

Department of Chemistry, Faculty of Sciences, University of Diyala, Diyala Governorate, Iraq.

***Corresponding authors:** aroo977@gmail.com

Original Research

Received:
19 April 2024
Revised:
12 June 2024
Accepted:
19 June 2024
Published online:
1 July 2024

Abstract:

In this research article, the Schiff base ligand 3-((2-amino-4-nitrophenyl) imino) indolin-2-one (Ln) was synthesized through the reaction between indoline 2, 3-dione and 4-nitrobenzene-1, 2-diamine. The synthesized ligand was then characterized using various analytical techniques, including ^{1}HNMR, UV-Vis, FT-IR, and element analysis C.H.N. The presence of nitrogen (N) and oxygen (O) atoms in the ligand structure makes it suitable for coordination chemistry. Furthermore, the ligand was employed for the synthesis of metal ion complexes by reacting it with transition metal salts such as $CoCl_2.6H_2O$, $NiCl_2.6H_2O$, $CuCl_2.2H_2O$, and anhydrous $ZnCl_2$. These metal (II) complexes were subsequently utilized for the oxidation of alcohols in toluene under thermal conditions. To further investigate the properties of the newly prepared complexes $[M(Ln^n)_2]Cl_2$, various characterization techniques, including FTIR, UV-Vis, magnetic susceptibility, atomic absorption spectroscopy, and molar conductance were employed. Moreover, this study aimed to evaluate the impact of the synthesized ligand and its complexes on the Mitotic Index in human lymphocyte cells. A concentration of 100 μg/mL was utilized, and the exposure time was set at 15 minutes. The results indicated that the ligand had a greater effect on the rate of lymphocyte cell division compared to the complexes. This suggests that the ligand exhibited a stronger resemblance to colchicine in terms of inhibiting lymphocyte division during the equatorial phase.

Keywords: Complexes; Indole; Isatin; Lymphocyte cells of humans; Oxidation

1. Introduction

The process of oxidizing alcohols to produce the corresponding aldehydes and ketones is of great significance in the field of synthetic organic chemistry [1–5]. This denotes a vital inclusion of key functional groups, such as aldehydes, ketones, and carboxylic acids. The conversion of alcohols into aldehydes and ketones through oxidation is a crucial process in both academic research and industrial applications [6, 7]. This transformation highlights the significant contribution of the carbonyl group in synthesis and its widespread occurrence in fine chemicals, pharmaceuticals, and fragrances. Indeed, these oxidations are considered to be among the most significant reactions in the field of medicinal chemistry [8, 9]. Historically, a stoichiometric quantity of a chromium salt, including CrO_3, PCC, and PDC, was utilized. Nevertheless, these chemicals pose a risk and may lead to time-consuming purification processes and an unnecessary impact on the environment. Consequently, there is a growing emphasis on catalytic oxidations utilizing transition metals. High catalytic activity and selectivity have been achieved through the utilization of certain homogeneous metal complexes of Pd [10–13], Ru [14–17], Os [18–21], Co [22], and Cu [23–25].

Therefore, a broad range of techniques have been devised. Efforts are currently underway to establish conditions that are environmentally sustainable. The objective of these endeavors is to carry out the oxidation of alcohols by utilizing cost-effective green oxidants like air, oxygen, hydrogen peroxide, tert-butyl hydrogen peroxide, and other metal-free

oxidants. This process is conducted in the presence of heterogeneous catalysts and environmentally friendly solvents, ensuring an eco-friendlier approach.

Schiff bases represent a category of ligands that find extensive utility in various applications [26–29]. The formation of Schiff base-metal complexes involves a combination of different ligands and metals, serving as catalysts in numerous chemical reactions. These catalysts have been employed in a diverse range of reactions including oxidation processes [29], C–C and C–O coupling reactions [30, 31], epoxidation reactions [32–35], and the synthesis of tetrazole rings [36]. Cancer is a serious and potentially fatal illness characterized by the proliferation of abnormal cells that have the capacity to rapidly spread throughout the body, leading to the destruction of healthy tissues [37]. These cells cluster together to form what is commonly referred to as a tumor. The biological activity of Schiff bases is believed to be significantly influenced by the C=N linkage, as suggested. Furthermore, extensive research has been conducted to investigate the chemical and biological significance associated with the existence of a solitary electron pair in a sp^2 hybridized orbital of the nitrogen atom within the azomethine group. Schiff bases and their coordination compounds play a crucial role in medicinal and pharmaceutical sectors due to their diverse array of biological functions, encompassing anti-malarial, antifungal, diuretic, anticancer, antibacterial, antiviral, insecticidal, antitumor, anti-inflammatory, anti-tuberculosis, and anti-HIV properties [38–41].

In this study, a new Schiff base ligand was synthesized by reacting indoline 2,3-dione with 4-nitrobenzene-1,2-diamine. The resulting ligand was then used to form metal ion complexes with Co, Ni, Cu, and Zn. These complexes were subsequently employed in the oxidation of alcohols. Furthermore, the impact of the synthesized complexes on the mitotic index of human lymphocytes was examined.

2. Experimental

2.1 Materials and Apparatus

The study utilized various materials, including Indoline-2,3-dione ($C_8H_5NO_2$, 99% purity, Aldrich), 4-nitrobenzene-1,2-diamine ($C_6H_7N_3O_2$, 98% purity, Fluka), high-quality absolute ethanol (99% purity, Scharlaw), Glacial acetic acid (CH_3COOH, 99.9% purity, BDH), Zinc chloride anhydrous ($ZnCl_2$, 99% purity, Sigma-Aldrich), Cobalt (II) chloride ($CoCl_2.6H_2O$, 96% purity, Sigma-Aldrich), Cupric (II) chloride ($CuCl_2.2H_2O$, 99% purity, ACS), and Nickel (II) chloride ($NiCl_2.6H_2O$, 99%, CDH). These materials were carefully selected for their specific properties and purities to ensure accurate and reliable results in the study. The study employed various instruments, including the SMP10 Melting Point apparatus, PERKIN ELMER SPEACTUM-65 FTIR spectrophotometer with a KBr disc in the range of 4000-400 cm^{-1}, PRUKUR 400 MHz ^{1}H-NMR spectrophotometer, and Shimadzu UV-160 A UV-Vis spectrophotometer. The measurements were carried out at room temperature using a quartz cell with a path length of 1.0 cm, covering a wavelength range from 200 to 900 nm. Additionally, elemental analysis was performed using the EM-017 mth instrument for C, H, and N analysis, Shimadzu Atomic Absorption 680 Flame Spectrophotometer for atomic absorption, and Balance Magnetic Susceptibility Model MSB-MKI for determining magnetic susceptibility through the Faraday method.

2.2 Synthesis of ligand 3-((2-amino-4-nitrophenyl) imino) indolin-2-one

In a solution of 0.8 g (5.4 mmol) of indoline 2,3-dione dissolved in 20 mL of ethanol, 0.83 g (5.4 mmol) of 4-nitrobenzene-1,2-diamine was added along with 20 mL of ethanol. Subsequently, 1 mL of glacial acetic acid was introduced into the reaction mixture. The resulting mixture was then refluxed for a duration of 4 hours at 78 °C in a water bath. Afterward, the reaction was left at room temperature for an extended period. The following day, the reaction mixture was filtered, washed with water, and dried in air. An orange precipitate was obtained with a yield of 87%. The melting point was recorded as 150-152°C. The calculated analysis for $C_14H_10N_4O_3$ (282.3) yielded the following percentages: C (59.57), H (3.57), and N (19.85). The experimental analysis showed the following percentages: C (59.77), H (3.66), N (19.96). The 1HNMR spectrum (400 MHz, DMSO-d_6) displayed peaks at δ (ppm): 11.23 (s, 1H, NH), 7.68-6.79 (m, 7 H, Ar-H), and 6.46 (s, 2H, NH_2). The FTIR spectrum (cm^{-1}) exhibited peaks at 3454 and 3371 (NH_2), 3253 (NH), 3072 (CH aromatic), 1692 (CO), and 1625 (CN isomethane). The UV-Vis spectrum (cm^{-1}) displayed peaks at ($\pi \longrightarrow \pi^*$ = 36231 and 29498) and (n$\longrightarrow \pi^*$ = 28985).

2.3 Synthesis of metal complexes

The $[M(Ln^n)_2]Cl_2$ transition metal complexes were synthesized through the combination of one equivalent of transition metal ions, dissolved in 10 mL of ethanol, with two equivalents of the ligand (0.2 g, 0.7 mmol) dissolved in 20 mL of ethanol. Following this, a few drops of 5% KOH were introduced to the mixture, which was then refluxed. The reaction mixture was subjected to a water bath maintained at 78 °C for a period of two hours. Subsequently, the solvent underwent partial evaporation, leading to the formation of a precipitate that was filtered, washed with water, and air-dried.

2.4 General procedure for the oxidation of alcohols

The product was obtained by charging a 10-mL round-bottom flask with various alcohols (5.0 mmol), a catalyst (1.5 mol%, 80 mg), cyclohexanone (2.5 mmol), and 1.5 mL of toluene as a solvent. The resulting mixture was stirred under reflux for an appropriate duration. Subsequently, the volatile components were removed under reduced pressure, and the remaining residue was purified using flash chromatography over silica gel. Ethyl acetate/petroleum ether was employed as the eluent during the purification process.

2.5 Investigation of prepared complexes on lymphatic cell division in human blood

The effect of both the ligand and its complexes on lymphocytes was investigated through short-term culture, following the methodology described by Verma and Babu [42]. Blood samples were collected randomly from individuals of differ-

ent age groups using a medical syringe filled with a 5 mL heparin solution for each participant. These blood samples were utilized in the subsequent experiments.

2.6 Transplantation of Blood and prepared compound

Incorporate 0.2 mL of each complex into the complete plant medium PMRI-1640, considering the total volume of the mixture. Subsequently, 0.5 mL of blood was introduced into each tube using a 5 mL syringe. Following this step, add 0.1 mL of lymphocytes and blend with the medium, then incubate at a tilted angle at 37 °C for 72 hours, ensuring to mix the contents of the tubes every 12 hours. Reserve one of the tubes without the addition of any prepared compound to serve as the control for this experiment.

2.7 Harvesting of Cell

In the control tube, a 0.1 mL volume of colchicine with a concentration of 100 μg/mL was added 15 minutes prior to the conclusion of the initial culture period. Conversely, the treated tubes did not receive any colchicine. Subsequently, all tubes were returned to the incubator. After the incubation period, the tubes were centrifuged at 1500 rpm for 10 minutes, resulting in the removal of the liquid portion above the sediment (supernatant). The resulting sediment was thoroughly mixed with the remaining culture medium. Gradually, 5-10 mL of a 0.075 M hypotonic solution was added to each tube while gently warming and intermittently shaking the tubes using a water bath set at 37°C for a duration of 30 minutes. Following this, the tubes were subjected to centrifugation for 10 minutes at 1500 rpm, and the liquid portion above the sediment was discarded.

2.8 Fixation, washing, dropping, pigmentation, microscopy, and mitotic index

The fixation procedure was repeated until the suspension displayed a distinct color. Following this, the precipitate was re-suspended by introducing 1 mL of the fixative, and the resulting mixture was then stored at -20 °C. Clean, cool, and dry glass slides were readied, and the cells were thoroughly mixed before being carefully dropped onto the chilled slides using a Pasteur pipette from a distance of 0.5-1 m. The slides were allowed to air dry. Afterward, they were stained with a Giemsa stain that had been prepared in a warm Sorensen buffer solution at a ratio of 4:1 for a duration of 2-3 minutes, rinsed with Sorensen buffer, and left to dry. The stained slides were examined under light microscopy to determine the Mitotic Index (MI), which is calculated by dividing the number of cells in metaphase by the total number of cells examined (1000), as shown in the equation below [43]:

*Mitotic Index (MI) = {number of dividing cells The total number of cells is 1000} *100*

Statistical analysis

The results underwent statistical analysis using the Duncan Multiplex experiment, with significant differences observed at a probability level of $P < 0.05$.

Spectroscopic and physical data of the synthesized metal complexes

Complex of $[Co(L^n)_2]Cl_2$: 80% brown precipitate; m.p (198-200 °C) decomposition; Anal. Calc. for $C_28H_20Cl_2CoN_8O_6$ (694.3), C (48.43), H (2.90), N (16.14), Co (8.49), Found C (48.17), H (2.72), N (16.55), Co (8.00); μeff (B.M) = 4.11; Λ in DMSO solvent = 75 $cm^2.ohm^{-1}.mol^{-1}$; FT-IR spectrum (cm^{-1}): 3436 and 3349 (NH_2), 3216 (NH), 3092 (CH aromatic),1649 (CO), 1629 (CN azomethine), 662 (Co-N), 409 (Co-O); UV-Vis (cm^{-1}): Intra ligand= 35587 and 29850, ν_3= $^4T_{1g(F)} \longrightarrow {}^4T_{1g.(p)}$= 23584, ν_2= $^4T_{1g(F)} \longrightarrow {}^4A_{2g\,(F)}$ =13477.

Complex of $[Ni(L^n)_2]Cl_2$: 85 % black precipitate; m.p (200-203 °C) decomposition; Anal. Calc. for $C_28H_20Cl_2NiN_8O_6$ (694.1), C (48.45); H (2.90); N (16.14); Ni 8.46, Found: C 48.60; H 3.01; N 16.41; Ni 8.71; μeff (B.M) = 2.89; Λ in DMSO solvent = 72 $cm^2.ohm^{-1}.mol^{-1}$; FT-IR spectrum (cm^{-1}): 3435 and 3342 (NH_2), 3219 (NH), 3091(CH aromatic), 1727 (CO), 1618 (CN asomethine),618 (Ni-N), 455(Ni-O); UV-Vis (cm^{-1}): Intra ligand= 35971 and 28985, ν_3= $^3A_{2g} \longrightarrow {}^3T_{1g(p)}$= 24038, ν_2=$^3A_{2g} \longrightarrow {}^3T_{1g(F)}$= 12531, ν_1=$^3A_{2g} \longrightarrow {}^3T_{2g(F)}$=11876.

Complex of $[Cu(L^n)_2]Cl_2$: 80 % black precipitate; m.p (210-213 °C) decomposition; Anal. Calc. for $C_28H_20Cl_2CuN_8O_6$ (699.0), C (48.11); H (2.88); N (16.03); Cu (9.09), Found: C 48.33; H 3.11; N 16.35; Cu 9.66; μeff (B.M) = 1.77; Λ in DMSO solvent = 77 $cm^2.ohm^{-1}.mol^{-1}$; FT-IR spectrum (cm^{-1}): 3435 and 3330 (NH_2), 3220 (NH), 3098(CH aromatic), 1721 (CO), 1611 (CN asomethine), 644 (Cu-N), 489 (Cu-O); UV-Vis (cm^{-1}): Intra ligand= 36363 and 26455, ν= $^2Eg \longrightarrow {}^2T_{2g}$=16666.

Complex of $[Zn(L)^n{}_2]Cl_2$: 81 % light brown precipitate; m.p (180-183 °C) decomposition; Anal. Calc. for $C_28H_20Cl_2ZnN_8O_6$ (700.8), C (47.99); H (2.88); N (15.99); Zn (9.33), Found: C 48.09; H 3.08; N 16.28; Zn 9.85; μeff = 0.00 B.M; Λ in DMSO solvent = 80 $cm^2.ohm^{-1}.mol^{-1}$; FT-IR spectrum (cm^{-1}): 3451 and 3351 (NH_2), 3227 (NH), 3051(CH aromatic), 1707 (CO), 1619 (CN asomethine), 617 (Zn-N), 419 (Zn-O); UV-Vis (cm^{-1}): Intra ligand= 37313, 27548 and 24038.

3. Result and Discussion

3.1 Synthesis of ligand

The synthetic route (Scheme 1) was employed to prepare the ligand Schiff base 3-((2-amino-4-nitrophenyl)imino)indolin-2-one. The prepared ligand was characterized by some techniques such as (C, H, N), ^{1}H NMR, FT-IR, and UV-vis spectroscopy.

Fig. 1 illustrates the ^{1}H-NMR spectrum of a ligand, which displayed a single signal at 11.23 ppm corresponding to the proton of the indole ring (NH). Furthermore, the signals observed in the range of 7.68-6.79 ppm can be attributed to the protons of an aromatic ring. Additionally, the signals at 6.46 ppm can be assigned to two protons of the amine group [44]. Consequently, the number of hydrogen atoms detected in the NMR spectrum aligns with the number of hydrogen atoms present in the proposed structure of the synthesized ligand.

3.2 Synthesis and characterization of metal (II) complexes

Upon completion of the synthesis of ligand Schiff base 3-((2-amino-4-nitrophenyl)imino)indolin-2-one, the metal

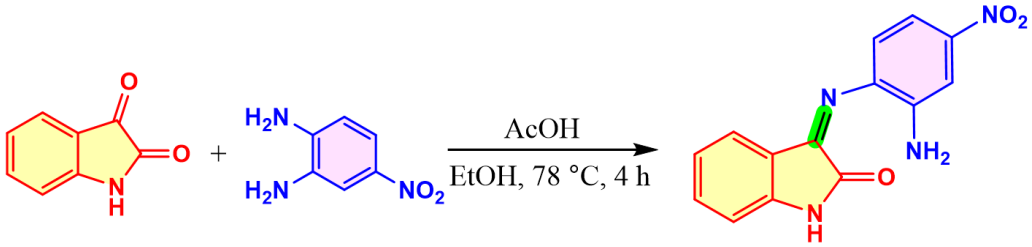

Scheme 1. A synthetic pathway for the preparation of ligand.

complexes were synthesized via the described method (Scheme 2). It is evident that each of the complexes underwent reflux in ethanol with the addition of 5% KOH and the corresponding metal salts $CoCl_2.6H_2O$, $NiCl_2.6H_2O$, $CuCl_2.2H_2O$, and anhydrous $ZnCl_2$ to yield the Co (II), Ni (II), Cu (II), and Zn (II) complexes, respectively. The prepared complexes were characterized using FT-IR, UV-Vis, magnetic susceptibility, atomic absorption spectroscopy, and molar conductance. Fig. 2 illustrates the FT-IR spectrum of the ligand, exhibiting absorption bands at 3454 cm^{-1} and 3371 cm^{-1}, which indicate the stretching vibration of the N–H bond in the NH_2 group. Moreover, a band at 3253 cm^{-1} corresponds to the stretching vibration of NH in the indole ring. The presence of absorption bands at 1692 cm^{-1} is attributed to the stretching vibration of a carbonyl group. Furthermore, an absorption band emerges at 1625 cm^{-1}, indicating the presence of the azomethine CH=N group [45, 46]. The observed absorption bands confirm the structure of the L^n ligand. The synthesized complexes' infrared spectra exhibit noticeable shifts in the stretching vibrations of the (NH_2), (CO), and (CN) azomethine groups compared to the spectrum of the free ligand. These shifts provide compelling evidence for coordination through the nitrogen atom of the azomethine group, the nitrogen atom of the amine group, and the oxygen atom of the carbonyl group from the ligand to the metal ion. Additionally, new weak intensity bands appear in the range of (617-662) cm^{-1}, indicating the stretching vibration of M-N, and in the range of (409-489) cm^{-1}, indicating the stretching vibration of M-O for the complexes [47]. The experimental section provides a detailed illustration of the Infrared spectra data for both the synthesized compounds. The UV-Vis spectra of ligands and synthesized of metal complexes are shown in Fig. 3.The ligand UV-Vis spectrum exhibited three bands at 276, 339, and 345 nm, corresponding to $\pi \longrightarrow \pi^*$, $\pi \longrightarrow \pi^*$, and $n \longrightarrow \pi^*$ electronic transitions, respectively. Conversely, the complexes' spectra displayed shifts in the bands' positions compared to the free ligand, accompanied by the appearance of new low-intensity bands in the visible region. These additional bands were attributed to d-d transitions,

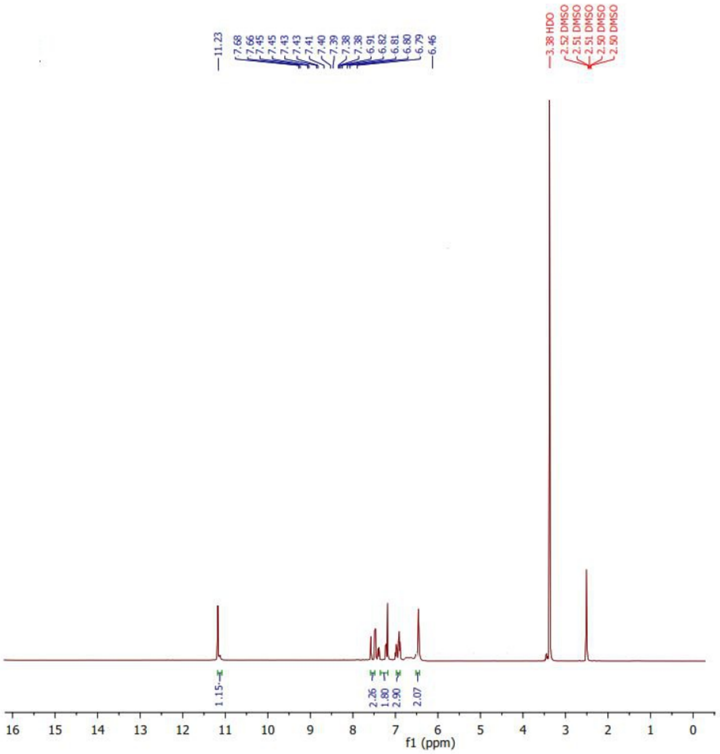

Figure 1. ^{1}HNMR spectrum of Schiff base ligand.

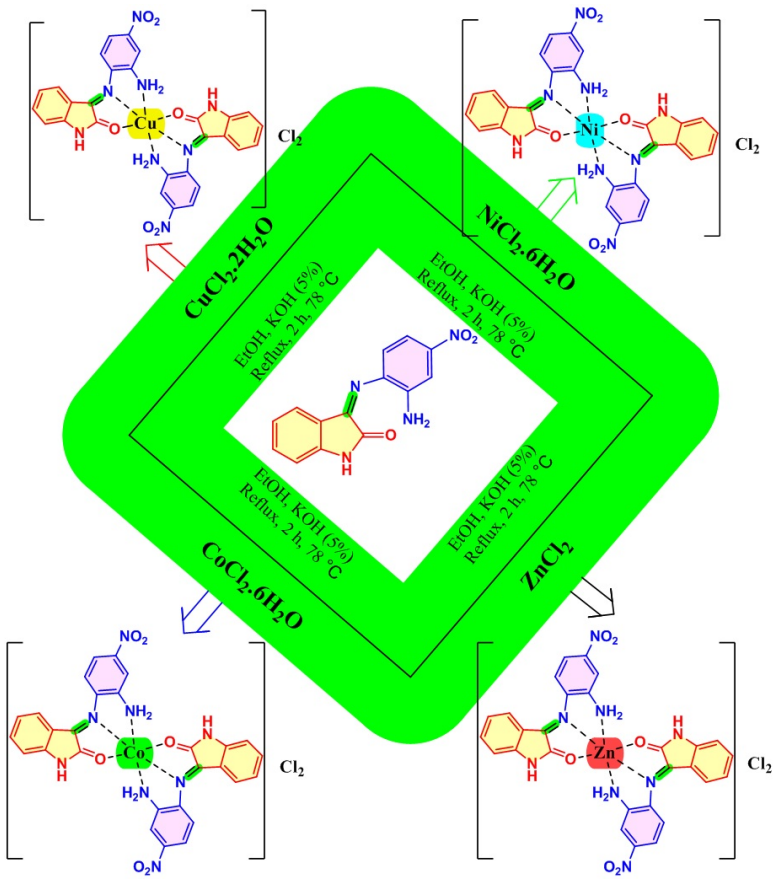

Scheme 2. General routes for the preparation of Schiff base metal (II) complexes.

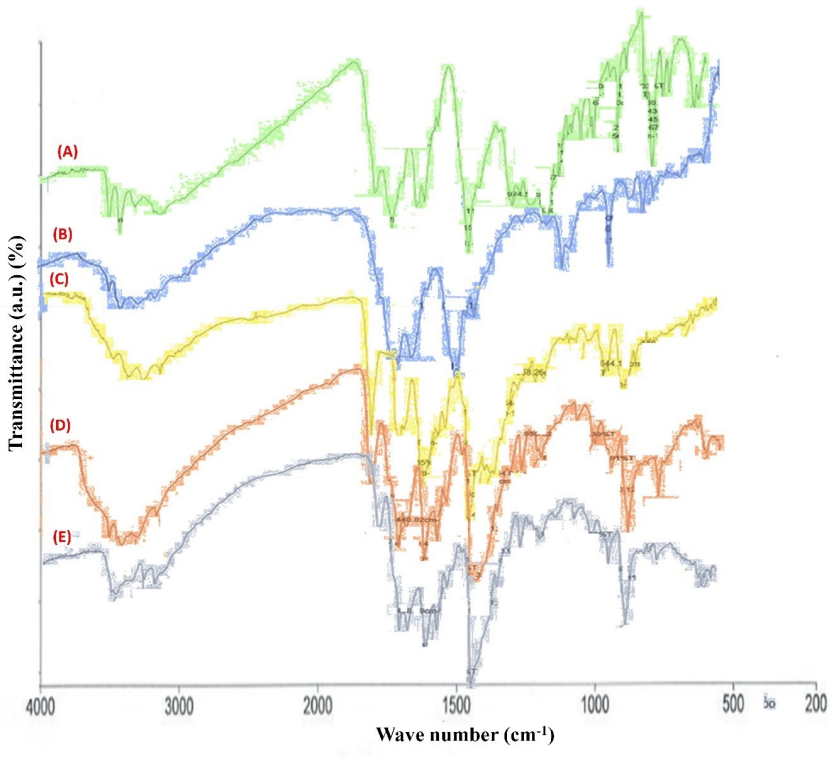

Figure 2. FT-IR spectra of (A) ligand, (B) Co (II) complex, (C) Cu (II) complex, (D) Ni (II) complex, (E) Zn (II) complex.

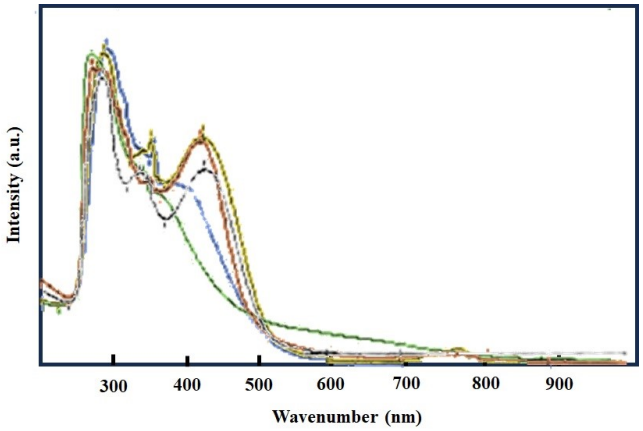

Figure 3. UV-Vis spectra of Ligand (blue), Ni-complex (yellow), Cu-complex (green), Co-complex (Red), and Zn-complex (black).

providing proof of metal-ligand coordination and complex formation. Notably, the $[Zn(L^n)_2]Cl_2$ complex did not show an absorption band in the (400-900) nm range, indicating the absence of d-d electronic transitions in the visible region due to its d^{10} system. Nevertheless, a slight change in band positions relative to those of the free ligand supported the coordination between Zn and the ligand. The experimental section presents the UV-Vis spectra data, along with their assigned transitions, for the synthesized compounds in this investigation [48–50].

Four complexes were synthesized through the reaction of the L^n ligand with Co (II), Ni (II), Cu (II), and Zn (II). To characterize these complexes, elemental analysis, molar conductivity, atomic absorption, and magnetic susceptibility techniques were employed. The experimental results, as presented in the experimental section, demonstrate that both elemental analysis and atomic absorption support the proposed structures of the synthesized complexes. The molar conductivity values of the complexes fall within the range of (72-80) $cm^2.ohm^{-1}.mol^{-1}$, indicating their conductive nature with a 1:2 ratio. This suggests that both chloride ions are situated outside the coordination sphere in the complexes, thereby confirming the suggested structures $[M(C_14H_10N_4O_3)_2]Cl_2$. On the other hand, the magnetic susceptibility data reveal that the complexes exhibit paramagnetic properties. Specifically, the Cu (II) complex has a μeff value of 1.77, the Ni (II) complex has a μeff value of 2.89, and the Co (II) complex has a μeff value of 4.11. These values indicate that the complexes possess a high-spin octahedral structure. In contrast, the Zn (II) complex exhibits nonmagnetic properties [51].

3.3 Catalytic evaluation of metal (II) complexes for oxidation of alcohols0

At the outset, a series of test reactions were conducted utilizing 1-phenylethanol as a representative substrate (Table 1). By conducting various experiments, we have discovered that the reaction can be effectively conducted by employing alternative metal (II) complexes along with a highly donating bisphosphine known as 1,2-bis(dicyclohexylphosphino)ethane (dcype). Acetophenone was achieved in almost complete yield through the use of this system, where the corresponding alcohol in toluene was subjected to reflux with cyclohexanone as the hydride acceptor. Initially, different solvents, including dichloromethane, chloroform, THF, 1,4-dioxane, DMF, acetonitrile, and toluene, were evaluated for the model reaction (Table 1, entries 1-8). As can be obtained during these tests, the toluene solvent shows the best result for oxidation of 1-phenylethanol to corresponding product. In continueing the optimization of the model reaction, various hydride acceptor such as cyclohexanone, acetone, 1,1,1-trifluoroacetone, and without hydride acceptor were applied, and cyclohexanone was the best choice for this parameter (Table 1, entries 9-11). In order to show the efficiency of different prepared catalysts, all of these catalysts were investigated (Table 1, entries 12-14). During the initial screening studies, Ni (II) and Cu (II) complexes demonstrated higher efficacy compared to the other metal (II) complexes that were tested. Finally, the amount of catalyst was checked, and 80 mg of catalyst was the optimum amount of metal complex (Table 1, entries 15-16) A wide range of secondary benzylic alcohols were examined under the most favorable reaction conditions (Scheme 3). In accordance with Scheme 3, various para-substituted acetophenone derivatives, regardless of the electron-withdrawing or electron-donating para-substituents on the aryl ring, underwent smooth reactions to produce the respective ketones. The desired product, 3-pyridylethanol, was obtained with successful yields of 94%, 92%, 90%, and 88% using Ni, Cu, Co, and Zn catalysts, respectively. Furthermore, the current approach demonstrated compatibility with substrates such as 1-(1-Naphthyl)ethanol, 1,1-diphenylmethanol, and 1,1-(4,4-dicyanodiphenyl)methanol. Based on these observations, we propose that the metal-catalyzed transfer dehydrogenation commences by displacing the nitrogen and oxygen atom donor in one of the ligands on the metal-complex with an alcohol moiety. This displacement occurs simultaneously with the formation of the alkoxide-nickel intermediate (I) (Scheme 4). Subsequently, the alcohol molecule captures a proton, leading to the loss of H_3O^+. This particular step is anticipated to be facilitated by the presence of electron-rich ligands that enhance the electron density around the

Table 1. Optimization of the oxidation of 1-phenylethanol[a].

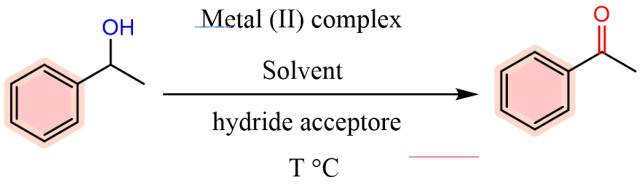

Entry	Type of Catalyst	Solvent	T (°C)	Amount of catalyst (mg)	Hydride acceptor	Conversion (%)[b]	Yield (%)[c]
1	Ni (II)	CH_2Cl_2	Reflux	80	cyclohexanone	15	20
2	Ni (II)	$CHCl_3$	Reflux	80	cyclohexanone	25	45
3	Ni (II)	THF[d]	Reflux	80	cyclohexanone	50	65
4	Ni (II)	1,4-dioxane	Reflux	80	cyclohexanone	20	25
5	Ni (II)	DMF[e]	Reflux	80	cyclohexanone	15	20
6	Ni (II)	CH_3CN	Reflux	80	cyclohexanone	45	65
7	Ni (II)	Toluene	Reflux	80	cyclohexanone	100	96
8	Ni (II)	Solvent-free	Reflux	80	cyclohexanone	10	10
9	Ni (II)	Toluene	Reflux	80	acetone	70	60
10	Ni (II)	Toluene	Reflux	80	1,1,1-trifluoroacetone	80	89
11	Ni (II)	Toluene	Reflux	80	none	10	15
12	Cu (II)	Toluene	Reflux	80	cyclohexanone	95	95
13	Co (II)	Toluene	Reflux	80	cyclohexanone	95	85
14	Zn (II)	Toluene	Reflux	80	cyclohexanone	95	90
15	Ni (II)	Toluene	Reflux	70	cyclohexanone	100	85
16	Ni (II)	Toluene	Reflux	90	cyclohexanone	90	80

a) General reaction conditions: alcohol (5.0 mmol), solvent (1.5 mL), hydride acceptor (2.5 mL). b) conversion of reaction was measured using GC in the presence of tetraline as an internal standard c) the yield of each reaction was measured based on the conversion of starting materials using GC. d) tetrahydrofuran e) dimethylformamide.

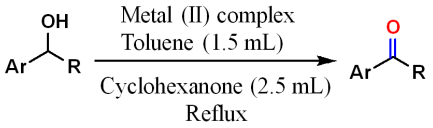

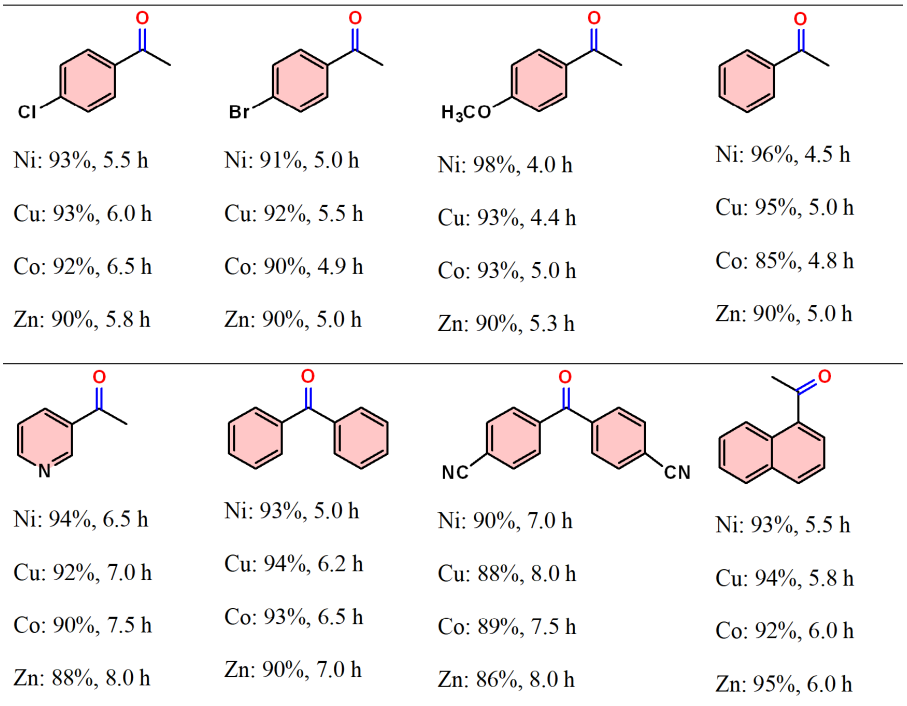

Scheme 3. Generality of the presented method and substrate scope of different alcohols to corresponding ketones.

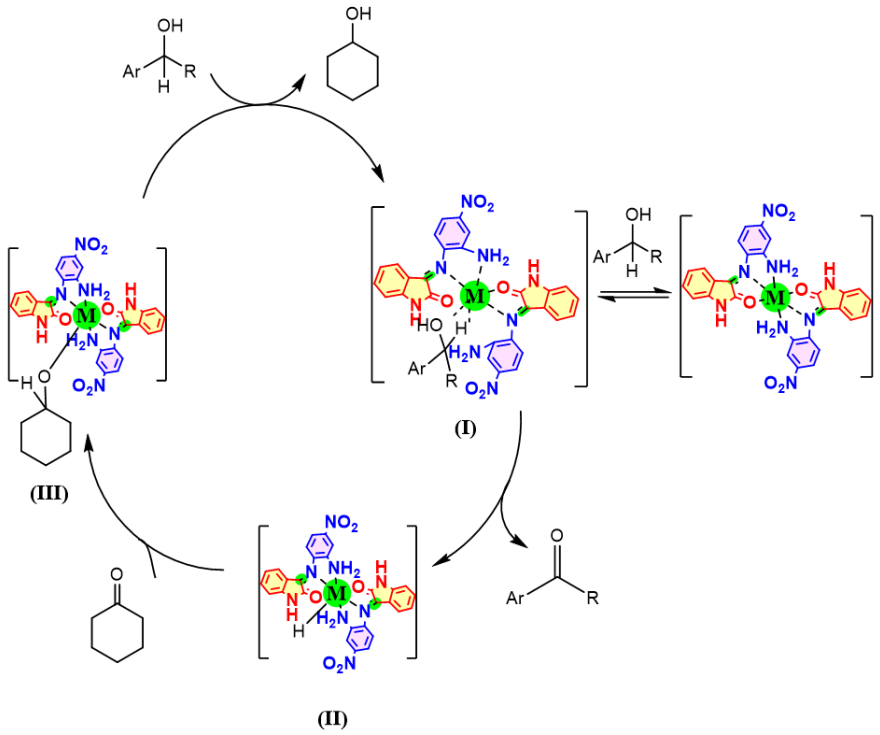

Scheme 4. Generality of the presented method and substrate scope of different alcohols to corresponding ketones.

metal. Following this, beta-elimination from (I) generates the desired ketone product while simultaneously producing a metal-hydride complex (II). The resulting hydride complex can be then inserted into cyclohexanone, forming alkoxide-metal (III). Further exchange with a molecule of the alcohol results in the formation of cyclohexanol and (I), thereby initiating a second cycle. Furthermore, an assessment was conducted to evaluate the reusability and recoverability of the catalysts containing metal (II) complexes in the oxidation process of 1-(4-methoxyphenyl)ethanol, resulting in the formation of the corresponding substituted acetophenoe (Fig. 4). The findings indicate that the metal (II)-complex catalysts were able to be reused for 8 cycles without a notable decrease in catalytic activity.

Table 2 presents a comparison of the effective application of this protocol in the oxidation of alcohols reaction. The suggested catalysts exhibit durability and outperform certain catalytic systems that have been previously reported,

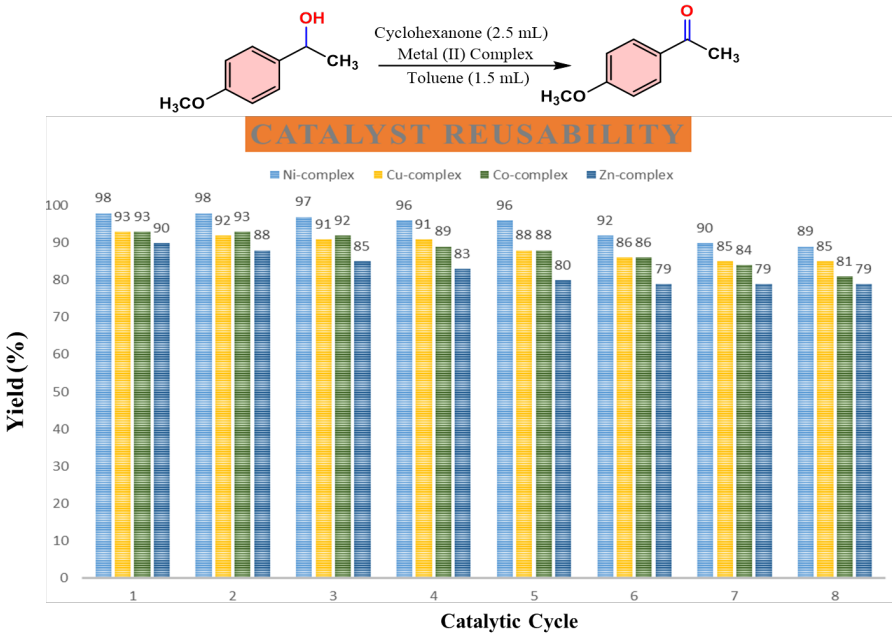

Figure 4. The catalytic reusability of used metal (II) complexes in the oxidation of 1-(4-methoxyphenyl)ethanol.

Table 2. A comparison study for the oxidation of secondary alcohols.

Entry	Catalyst	T (°C)	Solvent	Time (h)	Yield (%)	Ref.
1	CuAlO(OH)	27	Orthoiodic acid/LiOH	12	83	[52]
2	Cu (II) bromide	30	Special ligand/$NaOCH_3$/CH_3CN	5.5	92	[53]
3	Cu (II) nitrate	-	Silicagel/CCl_4	6.0	100	[54]
4	$C_38H_32Cu_2N_4O_10S_2$	100	Tert-butylhydroperoxide/H_2O	4.3	91	[55]
5	Cu (II) complex	Reflux	Toluene/cyclohexanone	4.4	93	This work

including recoverable catalytic systems.

3.4 The impact of the synthesized complexes on lymphatic cell division in human blood

Fig. 5 illustrates the impact of Colchicine, along with the synthesized complexes, on the metastasis of human blood Lymphatic Cell. The blocked cell ratios in metaphase at concentrations of 100 at 15 minutes were 4.33%, 4.90%, 2.79%, 3.20%, 1.57%, and 2.34% for Colchicine, L^n, $[Co(L^n)_2]Cl_2$, $[Ni(L^n)_2]Cl_2$, $[Cu(L^n)_2]Cl_2$, and $[Zn(L^n)_2]Cl_2$ respectively, as detailed in Table 3. The findings indicated that the complexes exhibited favorable percentages compared to the control, particularly the Nickel complex, although they were lower than the control ratio in comparison to the ligand. This discrepancy was attributed to the presence of free groups like azomethine, ammine, and carbonyl in the ligand. Moreover, the control percentage over human lymphocyte cell line division was nearly identical in both the ligand and colchicine [56].

4. Conclusions

In conclusion, the ligand (L^n) in this investigation was synthesized by reacting isatine and 4-nitrobenzene-1, 2-diamine. This ligand exhibits tridentate behavior in coordination, binding with metal ions through the nitrogen atom of the azomethine group, the nitrogen atom of the amine group, and an oxygen atom of the carbonyl group. Conductivity measurements indicated that all the synthesized complexes possessed an ionic nature with a 1:2 ratio. Moreover, the prepared catalysts were effectively employed in the oxidation of secondary aromatic alcohols to their corresponding ketones. Additionally, the biological

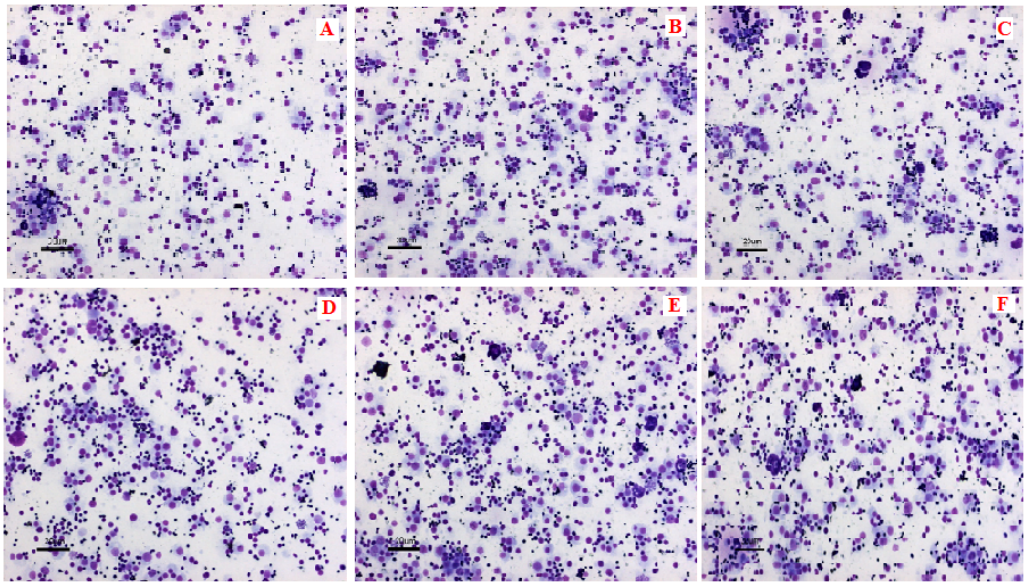

Figure 5. Humans lymphocytes in metaphase treatment with (A) Colchicine, (B) L^n, (C) $[Co(L^n)_2]Cl_2$, (D) $[Ni(L^n)_2]Cl_2$, (E) $[Cu(L^n)_2]Cl_2$, (F) $[Zn(L^n)_2]Cl_2$ in concentration 100 μg/mL.

Table 3. Effect of ligand and its complexes on Lymphatic Cell division in Human Blood.

Compound in concentration 100 μg/mL	Mitotic Index (MI %) M±SD
Colchicine	4.33 ± 0.01 a
L^n	4.90 ± 0.15 a
$Co(L^n)_2Cl_2$	2.79 ± 0.11 c
$Ni(L^n)_2Cl_2$	3.20 ± 0.15 b
$Cu(L^n)_2Cl_2$	1.57 ± 0.10 d
$Zn(L^n)_2Cl_2$	2.34 ± 0.08 c

activity evaluation of the ligand and its complexes on the Mitotic Index in human lymphocyte cells, with a 15-minute exposure time, demonstrated an increasing inhibition rate in the following order: $[Cu(L^n)_2]Cl_2 < [Zn(L^n)_2]Cl_2 < [Co(L^n)_2]Cl_2 < [Ni(L^n)_2]Cl_2 < L^n$. This suggests that the ligand exhibited the highest effectiveness and closely resembled colchicine in halting lymphocyte division during the equatorial phase.

Acknowledgments
The authors extend their gratitude and appreciation to the Chemistry Department at the University of Diyala in the College of Science, along with the Iraqi Center for Cancer and Medical Genetic Research at Mustansiriyah University, for their unwavering support throughout the completion of this study.

Authors Contributions
Authors have equal contribution role in preparing the paper.

Availability of Data and Materials
The data that support the findings of this study are available from the corresponding author upon reasonable request.

Conflict of Interests
The authors declare that they have no known competing financial interests or personal relationships that could have appeared to influence the work reported in this paper.

References

[1] K.E. Pfitzner and J.G. Moffatt. A new and selective oxidation of alcohols. *Journal of the American Chemical Society*, **85**(1963):3027–3028. DOI: https://doi.org/10.1021/ja00902a036.

[2] S. Najafishirtari, K. Friedel Ortega, M. Douthwaite, S. Pattisson, G.J. Hutchings, C.J. Bondue, K. Tschulik, D. Waffel, B. Peng, M. Deitermann, G.W. Busser, M. Muhler, and M. Behrens. A perspective on heterogeneous catalysts for the selective oxidation of alcohols. *Chemistry – A European Journal*, **27**(2021):16809–16833. DOI: https://doi.org/10.1002/chem.202102868.

[3] H. Alamgholiloo, S. Rostamnia, K. Zhang, T.H. Lee, Y.S. Lee, R.S. Varma, H.W. Jang, and M. Shokouhimehr. Boosting aerobic oxidation of alcohols via synergistic effect between tempo and a composite fe3o4/cu-bdc/go nanocatalyst. *ACS Omega*, **5**(2020):5182–5191. DOI: https://doi.org/10.1021/acsomega.9b04209.

[4] A. Guomundsson, K.E. Schlipkoter, and J.-E. Backvall. Iron(ii)-catalyzed biomimetic aerobic oxidation of alcohols. *Angew. Chem. Int. Ed.*, **59**(2020):5403–5406. DOI: https://doi.org/10.1002/anie.202000054.

[5] G. Lu, X. Huang, Y. Li, G. Zhao, G. Pang, and G. Wang. Covalently integrated core-shell mof@cof hybrids as efficient visible-light-driven photocatalysts for selective oxidation of alcohols. *Journal of Energy Chemistry*, **43**(2020):8–15. DOI: https://doi.org/10.1080/00304948.2020.1716624.

[6] D. Tang, G. Lu, Z. Shen, Y. Hu, L. Yao, B. Li, G. Zhao, B. Peng, and X. Huang. A review on photo-, electro- and photoelectro- catalytic strategies for selective oxidation of alcohols. *Journal of Energy Chemistry*, **77**(2023):80–118. DOI: https://doi.org/10.1016/j.jechem.2022.10.038.

[7] H. Yang, G. Li, G. Jiang, Z. Zhang, and Z. Hao. Heterogeneous selective oxidation over supported metal catalysts: From nanoparticles to single atoms. *Applied Catalysis B: Environmental*, **325**(2023):122384, . DOI: https://doi.org/10.1016/j.apcatb.2023.122384.

[8] V.J. Alli, P. Yadav, V. Suresh, and S.S. Jadav. Synthetic and medicinal chemistry approaches toward wee1 kinase inhibitors and its degraders. *ACS Omega*, **8**(2023):20196–20233. DOI: https://doi.org/10.1021/acsomega.3c01558.

[9] S.N. Carneiro, S.R. Khasnavis, J. Lee, T. W. Butler, J.D. Majmudar, C.W. am Ende, and N.D. Ball. Sulfur(vi) fluorides as tools in biomolecular and medicinal chemistry. *Organic & Biomolecular Chemistry*, **21**(2023):1356–1372. DOI: https://doi.org/10.1039/D2OB01891H.

[10] H. Keypour, J. Kouhdareh, S. Alavinia, R. Karimi-Nami, and İ. Karakaya. Pd-coordinated salinidol-modified mixed mof: An excellent active center for efficient nitroarenes reduction and selective oxidation of alcohols. *ACS Omega*, **8**(2023):22138–22149, . DOI: https://doi.org/10.1021/acsomega.3c02414.

[11] H. Keypour, J. Kouhdareh, S. Alavinia, R. Karimi-Nami, I. Karakaya, and K. Rabiei. Development of sustainable green catalysts for oxidation of alcohols via decorated palladium nanoparticles on magnetic carbon nanotube/mo. *J. Mol. Struct.*, **1294**(2023):136444, . DOI: https://doi.org/10.1016/j.molstruc.2023.136444.

[12] R. Nasiri, B. Gholipour, M. Nourmohammadi, Z. Karimi, S. Doaee, R. Taghavi, S. Rostamnia, E. Zarenezhad, F. Karimi, T. Kavetskyy, O. Smutok, A. Kiv, V. Soloviev, S. Khaksar, and A. S. Hamidi. Mesoporous hybrid organosilica for stabilizing pd nanoparticles and aerobic alcohol oxidation through pd hydride (pd–h2) species. *Int. J. Hydrogen Energy*, **48**(2023):6488–6498. DOI: https://doi.org/10.1016/j.ijhydene.2022.04.242.

[13] L. Zhao, O. Akdim, X. Huang, K. Wang, M. Douthwaite, S. Pattisson, R.J. Lewis, R. Lin, B. Yao, D.J. Morgan, G. Shaw, Q. He, D. Bethell, S. McIntosh, C.J. Kiely, and G.J. Hutchings. Insights into the effect of metal ratio on cooperative redox enhancement effects over au- and pd-mediated alcohol oxidation. *ACS Catalysis*, **13**(2023):2892–2903, . DOI: https://doi.org/10.1021/acscatal.2c06284.

[14] X. Dong, Y. Jia, M. Zhang, S. Ji, L. Leng, J. Hugh Horton, C. Xu, C. He, Q. Tan, J. Zhang, and Z. Li. Molten salt-induction of geometrically deformed ruthenium single atom catalysts with high performance for aerobic oxidation of alcohols. *Chem. Eng. J.*, **45**(2023):138660. DOI: https://doi.org/10.1016/j.cej.2022.138660.

[15] C.S. Ramirez-Barria, M. Isaacs, C. Parlett, K. Wilson, A. Guerrero-Ruiz, and I. Rodríguez-Ramos. Ru nanoparticles supported on n-doped reduced graphene oxide as valuable catalyst for the selective aerobic oxidation of benzyl alcohol. *Catal. Today*, **357**(2020):8–14. DOI: https://doi.org/10.1016/j.cattod.2019.05.057.

[16] J. Zhao, W.Y. Hernández, W. Zhou, Y. Yang, E.I. Vovk, M. Capron, and V. Ordomsky. Selective oxidation of alcohols to carbonyl compounds over small size colloidal ru nanoparticles. *ChemCatChem*, **12**(2020):238–247, . DOI: https://doi.org/10.1002/cctc.201901249.

[17] Q. Yang, T. Wang, Z. Zheng, B. Xing, C. Li, and B. Li. Constructing interfacial active sites in ru/g-c3n4-x photocatalyst for boosting h2 evolution coupled with selective benzyl-alcohol oxidation. *Applied Catalysis B: Environmental*, **315**(2022):121575, . DOI: https://doi.org/10.1016/j.apcatb.2022.121575.

[18] T. Ishizuka, H. Sugimoto, S. Itoh, and T. Kojima. Recent progress in oxidation chemistry of high-valent ruthenium-oxo and osmium-oxo complexes and related species. *Coord. Chem. Rev.*, **466**(2022):214536. DOI: https://doi.org/10.1016/j.ccr.2022.214536.

[19] M.L. Buil, M.A. Esteruelas, S. Izquierdo, A.I. Nicasio, and E. Oñate. N–h and c–h bond activations of an isoindoline promoted by iridium- and osmium-polyhydride complexes: A non-innocent bridge ligand for acceptorless and base-free dehydrogenation of secondary alcohols. *Organometallics*, **39**(2020):2719–2731. DOI: https://doi.org/10.1021/acs.organomet.0c00316.

[20] G.B. Shul'pin and L.S. Shul'pina. Oxidation of organic compounds with peroxides catalyzed by polynuclear metal compounds. *Catalysts*, **11**(2021):186.

[21] T. Takeshima, K. Usui, K. Mori, T. Asai, K. Yasuda, S. Kuroda, and Y. Yumura. Oxidative stress and male infertility. *Reproductive Medicine and Biology*, **20**(2021):41–42. DOI: https://doi.org/10.1002/rmb2.12353.

[22] H. Li, Z. Zhao, J. Qian, and B. Pan. Are free radicals the primary reactive species in co(ii)-mediated activation of peroxymonosulfate? new evidence for the role of the co(ii)–peroxymonosulfate complex. *CEnvironmental Science & Technology*, **55**(2021):6397–6406. DOI: https://doi.org/10.1021/acs.est.1c02015.

[23] Z. Liu, Z. Shen, N. Zhang, W. Zhong, and X. Liu. Aerobic oxidation of alcohols catalysed by cu(i)/nmi/tempo system and its mechanistic insights. *Catal. Lett.*, **148**(2018):2709–2718. DOI: https://doi.org/10.1007/s10562-018-2485-2.

[24] N. Jiang and A.J. Ragauskas. Cu(ii)-catalyzed selective aerobic oxidation of alcohols under mild conditions, the journal of organic chemistry. *J. Clust. Sci*, **71**(2006):7087–7090. DOI: https://doi.org/10.1021/jo060837y.

[25] M.F. Semmelhack, C.R. Schmid, D.A. Cortes, and C.S. Chou. Oxidation of alcohols to aldehydes with oxygen and cupric ion, mediated by nitrosonium io. *Journal of the American Chemical Society*, **106**(1984):3374–3376. URL 10.1021/ja00323a064.

[26] A. Hameed, M. al Rashida, M. Uroos, S. Abid Ali, and K.M. Khan. Schiff bases in medicinal chemistry: a patent review (2010-2015). *Expert Opinion on Therapeutic Patents*, **27**(2017):63–79. DOI: https://doi.org/10.1080/13543776.2017.1252752.

[27] C.M. da Silva, D.L. da Silva, L.V. Modolo, R.B. Alves, M.A. de Resende, C.V.B. Martins, and Â. de Fátima. Schiff bases: A short review of their antimicrobial activities. *Journal of Advanced Research*, **2**(2011):1–8. DOI: https://doi.org/10.1016/j.jare.2010.05.004.

[28] R. Antony, T. Arun, and S.T.D. Manickam. A review on applications of chitosan-based schiff bases. *Int. J. Biol. Macromol.*, **129**(2019):615–633. DOI: https://doi.org/10.1016/j.ijbiomac.2019.02.047.

[29] A.L. Berhanu, Gaurav, I. Mohiuddin, A.K. Malik, J.S. Aulakh, V. Kumar, and K.-H. Kim. A review of the applications of schiff bases as optical chemical sensors, trac. *Trends Anal. Chem.*, **116**(2019):74–91. DOI: https://doi.org/10.1016/j.trac.2019.04.025.

[30] P. Das and W. Linert. Schiff base-derived homogeneous and heterogeneous palladium catalysts for the suzuki–miyaura reaction. *Coord. Chem. Rev.*, **311**(2016):1–23. DOI: https://doi.org/10.1016/j.ccr.2015.11.010.

[31] K. Dhara, K. Sarkar, D. Srimani, S.K. Saha, P. Chattopadhyay, and A. Bhaumik. A new functionalized mesoporous matrix supported pd(ii)-schiff base complex: an efficient catalyst for the suzuki–miyaura coupling reaction. *Dalton Transactions*, **39**(2010):6395–6402. DOI: https://doi.org/10.1039/C003142A.

[32] T. Maharana, N. Nath, H.C. Pradhan, S. Mantri, A. Routaray, and A.K. Sutar. Polymer-supported first-row transition metal schiff base complexes: Efficient catalysts for epoxidation of alkenes. *React. Funct. Polym.*, **171**(2022):105142. DOI: https://doi.org/10.1016/j.reactfunctpolym.2021.105142.

[33] M. Sedighipoor, A.H. Kianfar, W.A.K. Mahmood, and M.H. Azarian. Epoxidation of alkenes by an oxidovanadium(iv) tetradentate schiff base complex as an efficient catalyst with tert-butyl hydroperoxide. *Inorg. Chim. Acta*, **457**(2017):116–121. DOI: https://doi.org/10.1016/j.ica.2016.12.018.

[34] Y. Guo, L. Xiao, P. Li, W. Zou, W. Zhang, and L. Hou. Binuclear molybdenum schiff-base complex: An efficient catalyst for the epoxidation of alkenes. *Molecular Catalysis*, **457**(2019):110498. DOI: https://doi.org/10.1016/j.mcat.2019.110498.

[35] M. Mirzaee, B. Bahramian, and A. Amoli. Schiff base-functionalized boehmite nanoparticle-supported molybdenum and vanadium complexes: efficient catalysts for the epoxidation of alkenes. *Appl. Organomet. Chem.*, **29**(2015):593–600. DOI: https://doi.org/10.1002/aoc.3335.

[36] E. Mohammed Faraj and F. Hameed Jumaa. Preparation, diagnostics and biological evaluation of new schiff base and tetrazole derivatives. *Materials Today: Proceedings*, **49**(2022):3549–3557. DOI: https://doi.org/10.1016/j.matpr.2021.08.061.

[37] M.T. Kaczmarek, M. Zabiszak, M. Nowak, and R. Jastrzab. Lanthanides: Schiff base complexes, applications in cancer diagnosis, therapy, and antibacterial activity. *Coord. Chem. Rev.*, **370**(2018):42–54. DOI: https://doi.org/10.1016/j.ccr.2018.05.012.

[38] E. Yousif, A. Majeed, K. Al-Sammarrae, N. Salih, J. Salimon, and B. Abdullah. Metal complexes of schiff base: Preparation, characterization and antibacterial activity. *Arabian Journal of Chemistry*, **10**(2017):S1639–S1644. DOI: https://doi.org/10.1016/j.arabjc.2013.06.006.

[39] R.S. Joseyphus and M.S. Nair. Antibacterial and antifungal studies on some schiff base complexes of zinc(ii). *Mycobiology*, **36**(2008):93–98. DOI: https://doi.org/10.4489/MYCO.2008.36.2.093.

[40] E.M. Hodnett and W.J. Dunn. Structure-antitumor activity correlation of some schiff bases. *J. Med. Chem.*, **13**(1970):768–770. DOI: https://doi.org/10.1021/jm00298a054.

[41] X. Zhong, J. Yi, J. Sun, H.L. Wei, W.S. Liu, and K.B. Yu. Synthesis and crystal structure of some transition metal complexes with a novel bis-schiff base ligand and their antitumor activities. *European Journal of Medicinal Chemistry*, **41**(2006):1090–1092. DOI: https://doi.org/10.1016/j.ejmech.2006.05.009.

[42] R.S. Verma and A. Babu. Human chromosomes: manual of basic techniques. (1989):768–770. DOI: https://doi.org/10.1021/jm00298a054.

[43] I.H. Mohammed, G.H. Jaafar, M.H. Qaddoori, M.H. Abdulateef, and Z.T. Abud. Effect of extraction on rhamnus caroliniana plant in mice chromosome lymphocytes and microtubules hepg2 cancer cell line. *Biochemical & Cellular Archives*, **21**(2021):768–770. DOI: https://doi.org/10.1021/jm00298a054.

[44] A.A. Jarullah, W.B. Ali, and O.W. Mohammed. Synthesis and antibacterial evaluation of ligand 3-(2-amino-5-b-benzoyl-phenylimino)-1,3-dihydro-indol-2-one and its complexes with ions of co(ii), ni(ii), cu(ii), and zn(ii). *AIP Conference Proceedings*, **2475**(2023). DOI: https://doi.org/10.1063/5.0105189.

[45] R.M. Silverstein and G.C. Bassler. Spectrometric identification of organic compounds. *J. Chem. Educ.*, **39**(1962):546. DOI: https://doi.org/10.1021/ed039p546.

[46] K. Ismail, W. Ali, and A. Jarullah. Synthesis, characterization and antifungal activity of some indolo [2-3-b] quinoxaline derivatives. *Journal of Global Pharma Technology*, **12**(2020):727–736.

[47] A.T. Numan, K.A. Sanak, E.M. Atiyah, and S.A. Sadiq. Synthesis and characterization of new bidentate chalcone ligand type (no) and its mn^{II}, co^{II}, ni^{II} and cu^{II} complexes with study of their antibacterial activity. *Diyala Journal for Pure Sciences*, **11**(2015): 25–42.

[48] N.H. Al-Shaalan. Synthesis, characterization and biological activities of cu(ii), co(ii), mn(ii), fe(ii), and uo_2(vi) complexes with a new schiff base hydrazone: O-hydroxyacetophenone-7-chloro-4-quinoline hydrazone. *Molecules*, **16**(2011):8629–8645. DOI: https://doi.org/10.3390/molecules16108629.

[49] R.M. Issa, A.M. Khedr, and H.F. Rizk. Uv–vis, ir and ^{1}h nmr spectroscopic studies of some schiff bases derivatives of 4-aminoantipyrine. *pectrochimica Acta Part A: Molecular and Biomolecular Spectroscopy*, **62**(2005):621–629, . DOI: https://doi.org/10.1016/j.saa.2005.01.026.

[50] R.M. Issa, A.M. Khedr, and H. Rizk. 1h nmr, ir and uv/vis spectroscopic studies of some schiff bases derived from 2-aminobenzothiazole and 2-amino-3-hydroxypyridin. *J. Chin. Chem. Soc.*, **55**(2008):875–884, . DOI: https://doi.org/10.1002/jccs.200800131.

[51] B. Geeta, K. Shravankumar, P.M. Reddy, E. Ravikrishna, M. Sarangapani, K.K. Reddy, and V. Ravinder. Binuclear cobalt(ii), nickel(ii), copper(ii) and palladium(ii) complexes of a new schiff-base as ligand: Synthesis, structural characterization, and antibacterial activity. *Spectrochimica Acta Part A: Molecular and Biomolecular Spectroscopy*, **77**(2010):911–915. DOI: https://doi.org/10.1016/j.saa.2010.08.004.

[52] S.G. Babu, P.A. Priyadarsini, and R. Karvembu. Copper on boehmite: A simple, selective, efficient and reusable heterogeneous catalyst for oxidation of alcohols with periodic acid in water at room temperature. *Appl. Catal., A*, **392**(2011):218–224. DOI: https://doi.org/10.1016/j.apcata.2010.11.012.

[53] N. Mase, T. Mizumori, and Y. Tatemoto. Aerobic copper/tempo-catalyzed oxidation of primary alcohols to aldehydes using a microbubble strategy to increase gas concentration in liquid phase reactions. *Chem. Commun.*, **47**(2011):2086–2088. DOI: https://doi.org/10.1039/C0CC04377J.

[54] T. Nishiguchi and F. Asano. Oxidation of alcohols by metal nitrates supported on silica gel. *Tetrahedron Lett.*, **29**(1988):6265–6266. DOI: https://doi.org/10.1016/S0040-4039(00)82321-7.

[55] S. Hazra, L.M.D.R.S. Martins, M.F.C. Guedes da Silva, and A.J.L. Pombeiro. Sulfonated schiff base copper(ii) complexes as efficient and selective catalysts in alcohol oxidation: syntheses and crystal structures. *RSC Adv.*, **5**(2015):90079–90088. DOI: https://doi.org/10.1039/C5RA19498A.

[56] H. Chen and J. Rhodes. Schiff base forming drugs: mechanisms of immune potentiation and therapeutic potential, journal of molecular medicine. *Journal of Molecular Medicine*, **74**(1996):497–504. DOI: https://doi.org/10.1007/BF00204975.